Randall-Sundrum corrections to the width difference and *CP*-violating phase in B_s^0-meson decays

Florian Goertz and Torsten Pfoh

Institut für Physik (THEP), Johannes Gutenberg-Universität, D-55099 Mainz, Germany

(Received 24 June 2011; published 11 November 2011)

We study the impact of the Randall-Sundrum setup on the width difference $\Delta\Gamma_s$ and the *CP*-violating phase ϕ_s in the $\bar{B}_s^0$-B_s^0 system. Our calculations are performed in the general framework of an effective theory, based on operator product expansion. The results can thus be used for many new-physics models. We find that the correction to the magnitude of the decay amplitude Γ_{12}^s is below 4% for a realistic choice of input parameters. The main modification in the $\Delta\Gamma_s/\beta_s$-plane is caused by a new *CP*-violating phase in the mixing amplitude, which allows for a better agreement with the experimental results of the CDF and D0 Collaborations from $B_s^0 \to J/\psi\phi$ decays. The best-fit value of the *CP* asymmetry $S_{\psi\phi}$ can be reproduced, while simultaneously the theoretical prediction for the semileptonic *CP* asymmetry $A_{\rm SL}^s$ can enter the 1σ range.

DOI: 10.1103/PhysRevD.84.095016 PACS numbers: 12.60.−i, 13.25.Hw, 14.40.Nd

I. INTRODUCTION

Within the search for new physics (NP) in the decay of B_s^0-mesons, an important observable is the width difference $\Delta\Gamma_s \equiv \Gamma_L^s - \Gamma_H^s$ between the light and the heavy meson state. According to the above definition, $\Delta\Gamma_s$ happens to be positive in the standard model (SM). It can be computed from the dispersive and absorptive part of the $\bar{B}_s^0$-B_s^0 mixing amplitude, M_{12}^s and Γ_{12}^s. To leading order (LO) in $|\Gamma_{12}^s|/|M_{12}^s|$ one finds the simple relation [1,2]

$$\Delta\Gamma_s = -\frac{2\,\mathrm{Re}(M_{12}^s\Gamma_{12}^{s*})}{|M_{12}^s|} = 2|\Gamma_{12}^s|\cos\phi_s. \tag{1}$$

We define the relative phase ϕ_s between the mixing and the decay amplitude according to the convention

$$\frac{M_{12}^s}{\Gamma_{12}^s} = -\frac{|M_{12}^s|}{|\Gamma_{12}^s|}e^{i\phi_s}, \qquad \phi_s = \arg(-M_{12}^s\Gamma_{12}^{s*}), \tag{2}$$

for which the SM value is positive and explicitly given by $\phi_s^{\rm SM} = (4.2 \pm 1.4) \times 10^{-3}$ [3]. The combined experimental results of the CDF and D0 Collaborations differ from the SM prediction in the $(\beta_s^{J/\psi\phi}, \Delta\Gamma_s)$-plane by about 2σ [4], whereas the latest CDF results disagree by 1σ only [5]. Here, $\beta_s^{J/\psi\phi} \in [-\pi/2, \pi/2]$ is the *CP*-violating phase in the interference of mixing and decay, obtained from the time-dependent angular analysis of flavor-tagged $B_s^0 \to J/\psi\phi$ decays. In the SM it is given by [3,6]

$$\beta_s^{J/\psi\phi} = -\arg\left(-\frac{\lambda_t^{bs}}{\lambda_c^{bs}}\right) = 0.020 \pm 0.005, \tag{3}$$

with $\lambda_q^{bs} = V_{qb}V_{qs}^*$. In the presence of NP, $\Delta\Gamma_s$ will be modified [7,8]. We adopt the notation of [9] and extend the SM relations according to

$$\begin{aligned} M_{12}^s &= M_{12}^{s\rm SM} + M_{12}^{s\rm NP} = M_{12}^{s\rm SM}R_M e^{i\phi_M}, \\ \Gamma_{12}^s &= \Gamma_{12}^{s\rm SM} + \Gamma_{12}^{s\rm NP} = \Gamma_{12}^{s\rm SM}R_\Gamma e^{i\phi_\Gamma}. \end{aligned} \tag{4}$$

From (1) it follows that

$$\Delta\Gamma_s = 2|\Gamma_{12}^{s\rm SM}|R_\Gamma\cos(\phi_s^{\rm SM} + \phi_M - \phi_\Gamma), \tag{5}$$

where $\Delta\Gamma_s^{\rm SM} = (0.087 \pm 0.021)\ \mathrm{ps}^{-1}$ [10]. A further important observable is the semileptonic *CP* asymmetry $A_{\rm SL}^s = \mathrm{Im}(\Gamma_{12}^s/M_{12}^s)$. Including NP corrections, we find

$$A_{\rm SL}^s = \frac{|\Gamma_{12}^{s\rm SM}|}{|M_{12}^{s\rm SM}|}\frac{R_\Gamma}{R_M}\sin(\phi_s^{\rm SM} + \phi_M - \phi_\Gamma). \tag{6}$$

Within the SM, the leading contribution to the dispersive part of the $\bar{B}_s^0$-B_s^0 mixing amplitude appears at the one-loop level. If NP involves flavor-changing neutral currents (FCNCs) at tree-level, these give rise to sizable corrections to the mass difference $\Delta m_{B_s} \equiv M_H^s - M_L^s = 2|M_{12}^s|$ [1]. In the context of Randall-Sundrum (RS) scenarios [11], the corrections to M_{12}^s have been calculated in [12,13]. See also [14,15] for a first estimate.

On the other hand, the presence of tree-level FCNCs and right-handed charged-current interactions gives rise to new decay diagrams. However, the NP corrections to the absorptive part of the amplitude are suppressed by m_W^2/Λ^2 with respect to the SM contribution, where Λ is the NP mass scale. Thus, they are neglected in many NP studies. Recently, model-independent estimates on $A_{\rm SL}^s$ in the presence of heavy gluons have been presented in [16], taking into account modifications in Γ_{12}^s. NP contributions from electroweak (EW) penguin operators as well as right-handed charged currents have not been considered. We find that the former can compete with or even dominate contributions from QCD penguins within the minimal RS model [13,17], while parts of the latter tend to give the dominant contribution to $\Gamma_{12}^{s\rm RS}$ for the most natural choice of input parameters.

This paper is organized as follows. In the next section we briefly summarize the main features of the RS model. We distinguish between two variants, the minimal and the custodial RS model with protection of the $Zb_L\bar{b}_L$ vertex,

each with a brane-localized Higgs. Then we calculate the leading contributions to Γ_{12}^s in the presence of NP, where we restrict ourselves to operators which are expected to give the dominant corrections for the models at hand. A numerical scan across RS contributions is presented in Sec. IV. Here, we evaluate M_{12}^s and Γ_{12}^s for 10 000 appropriate random sets of input parameters. Important constraints arise from the $\bar{B}_s^0$-B_s^0 oscillation frequency, which corresponds to the mass difference Δm_{B_s}, and the observable ϵ_K. The results are presented in the $\Delta\Gamma_s/\beta_s$- as well as the $A_{\mathrm{SL}}^s/S_{\psi\phi}$-plane. We conclude in Sec. V. In a series of appendixes we collect analytic results for RS Wilson coefficients needed in our computations.

II. FEATURES OF THE RS MODEL

The RS model is formulated on a five-dimensional (5D) anti–de Sitter space. The compactified fifth dimension is an S^1/Z_2-orbifold, labeled by a dimensionless coordinate $\phi \in [-\pi, \pi]$. The usual 4D space-time is rescaled by a so-called warp factor, such that length scales depend on the position in the extra dimension. The whole (5D) space-time is called the bulk. The RS metric is given by

$$ds^2 = e^{-2kr|\phi|}\eta_{\mu\nu}dx^\mu dx^\nu - r^2 d\phi^2, \tag{7}$$

with $\eta_{\mu\nu} = \mathrm{diag}(1, -1, -1, -1)$. Here, k and r denote the curvature and the radius of the fifth dimension, which are of the order of the (inverse) Planck scale. The Z_2-parity identifies points (x^μ, ϕ) and $(x^\mu, -\phi)$ and thus gives rise to boundaries at $\phi = 0$ and π, which are called Planck/ultraviolet (UV) and TeV/infrared (IR) brane, respectively. The RS model solves the gauge hierarchy problem by suppressing mass scales on the IR-brane. Explicitly, one achieves

$$M_{\mathrm{IR}} \equiv e^{-L}M_{\mathrm{Pl}} \equiv \epsilon M_{\mathrm{Pl}} \approx M_W \tag{8}$$

for $L \equiv kr\pi \approx 37$ ($\epsilon = 10^{-16}$). Thus, the strong hierarchy between the Planck and the weak scale, M_{Pl} and M_W, is understood by gravitational red-shifting, if the Higgs field is localized on or near the IR-brane. An effective four-dimensional description is usually obtained via Kaluza-Klein (KK) decomposition, which replaces each 5D field by an infinite tower of massive 4D fields, each of them supplied with a so-called profile depending on ϕ. Even fields under Z_2 (which in addition obey Neumann boundary conditions on both branes) possess a massless zero mode, which can however receive a mass via coupling to the Higgs field. Those light modes are interpreted as the SM fields. The masses of the additional heavy KK modes are of the order of the scale $M_{\mathrm{KK}} \equiv k\epsilon \approx$ few TeV, which is identified with the cutoff Λ of the effective low-energy theory. For instance, the mass of the first KK gluon is given by $m^{(1)} \approx 2.45M_{\mathrm{KK}}$. Take care of the fact that some authors define M_{KK} as the mass of the first excitation. Explicit formulas for the fermion- and gauge-boson profiles were first given in [18–21], respectively. The warp factor can be used to generate fermion-mass hierarchies [18,19,22]. This is achieved by localizing the fields differently in the bulk by an appropriate choice of the doublet/singlet 5D mass parameters M_{Q_i/q_i}, which are often called bulk masses.

The appearance of tree-level FCNCs is caused by the modified interactions between gauge and matter fields, which now contain overlap integrals of the corresponding profiles. If the gauge field possesses a mass, the overlap is flavor (and KK mode) dependent, giving rise to FCNCs when changing from the weak interaction to the mass eigenbasis. A crucial observation is that these nonuniversal overlap integrals are exponentially suppressed for UV localized (i.e. light) fermions. This is known as RS-GIM mechanism [14,15]. Details about the couplings and overlaps within the minimal RS formulation, with an IR-brane Higgs and gauge and matter fields in the bulk, can be found in [17]. The famous custodial extension including a protection for the $Zb_L\bar{b}_L$ vertex [23,24] is treated in [25,26].

If one deals with SM-like quarks, it is convenient to expand the profiles in terms of v^2/M_{KK}^2, where $v \approx 246$ GeV is the Higgs vacuum expectation value. This involves the zero-mode profile evaluated at the IR-brane

$$F(c) = \mathrm{sgn}[\cos(\pi c)]\sqrt{\frac{1+2c}{1-\epsilon^{1+2c}}} \tag{9}$$

as a function of the bulk-mass parameters $c_{Q_i} = M_{Q_i}/k$ and $c_{q_i} = -M_{q_i}/k$ [17]. To LO in v^2/M_{KK}^2 the spectrum of the light down-type quarks corresponds to the eigenvalues of the effective Yukawa matrix

$$\begin{aligned} \boldsymbol{Y}_d^{\mathrm{eff}} &= \mathrm{diag}[F(c_{Q_i})]\boldsymbol{Y}_d\mathrm{diag}[F(c_{d_i})] \\ &= \frac{\sqrt{2}}{v}\boldsymbol{U}_d\mathrm{diag}[m_d, m_s, m_b]\boldsymbol{W}_d^\dagger. \end{aligned} \tag{10}$$

The mixing matrices $\boldsymbol{U}_d$ and $\boldsymbol{W}_d$ are most easily obtained by a singular-value decomposition of the left-hand side of the latter equality. From now on, we will refer to the first nontrivial order in the expansion in v^2/M_{KK}^2 (which we also apply for massive gauge bosons) as the zero-mode approximation (ZMA).

III. CALCULATION OF Γ_{12}^s

Within the SM, Γ_{12}^s is known to next-to-leading order (NLO) in QCD [3,27–32]. In this section, we calculate the leading contribution to Γ_{12}^s in the presence of NP. It is given by the hadronic matrix element of the transition amplitude, which converts $\bar{B}_s^0$ into B_s^0

$$\begin{aligned} \Gamma_{12}^s &= \frac{1}{2m_{B_s}}\langle B_s^0|\mathcal{T}|\bar{B}_s^0\rangle, \\ \mathcal{T} &= \mathrm{Disc}\int d^4x \frac{i}{2}T[\mathcal{H}_{\mathrm{eff}}^{\Delta B=1}(x)\mathcal{H}_{\mathrm{eff}}^{\Delta B=1}(0)]. \end{aligned} \tag{11}$$

Taking the discontinuity in the expression above projects out those intermediate states, that are on-shell. The leading correction to the SM result is given by the interference between SM and NP insertions. The framework of heavy-quark expansion allows for a systematic evaluation of the matrix element in powers of $1/m_b$. At the zeroth order, the momentum of the B-meson in its rest frame corresponds to the momentum of the bottom quark, while the strange-quark momentum is set to zero. At typical hadronic distances $x > 1/m_b$, the transition of $\bar{B}_s^0$ into B_s^0 is a local process. Thus, the matrix element can be expanded in terms of local $\Delta B = 2$ operators. QCD corrections are implemented by running the $\Delta B = 1$ operators from the matching scale down to the mass of the bottom quark. The leading SM contributions can be collected into matrix elements of the $\Delta B = 2$ operators

$$\begin{aligned} \mathcal{Q}_1 &= (\bar{s}_i b_i)_{V-A}(\bar{s}_j b_j)_{V-A}, \\ \mathcal{Q}_2 &= (\bar{s}_i b_i)_{S+P}(\bar{s}_j b_j)_{S+P}, \end{aligned} \tag{12}$$

where i and j denote color indices and a summation over repeated indices is always understood throughout this paper. The shorthand notation $V \pm A$ indicates the Dirac structure $\gamma^\mu(1 \pm \gamma^5)$ in between the spinors, whereas $S \pm P$ denotes $(1 \pm \gamma^5)$. The possibility of having right-handed charged currents within the RS model asks for further $\Delta B = 2$ operators, caused by interference of the SM with NP insertions. We introduce

$$\begin{aligned} \mathcal{Q}_3 &= (\bar{s}_i b_j)_{S+P}(\bar{s}_j b_i)_{S+P}, \\ \mathcal{Q}_4 &= (\bar{s}_i b_i)_{S-P}(\bar{s}_j b_j)_{S+P}, \\ \mathcal{Q}_5 &= (\bar{s}_i b_j)_{S-P}(\bar{s}_j b_i)_{S+P}. \end{aligned} \tag{13}$$

The appropriate $\Delta B = 1$ Hamiltonian, allowing for new right-handed charged currents as well as FCNCs, is given by

$$\begin{aligned} \mathcal{H}_{\text{eff}}^{\Delta B=1} = \frac{G_F}{\sqrt{2}} \lambda_c^{bs} \Bigg[\sum_{i=1,2} (C_i Q_i + C_i^{\text{LL}} Q_i + C_i^{\text{LR}} Q_i^{\text{LR}} \\ + C_i^{\text{RL}} Q_i^{\text{RL}}) + \sum_{i=3}^{10} C_i Q_i \Bigg] + \sum_{i=3}^{10} (C_i^{\text{NP}} Q_i + \tilde{C}_i^{\text{NP}} \tilde{Q}_i). \end{aligned} \tag{14}$$

In the RS model the operators $Q_{1,2}$ arise from (KK) $W^\pm$-boson exchange, and the LR/RL operators involve right-handed charged currents. They are defined as

$$\begin{aligned} Q_1 &= (\bar{s}_i c_j)_{V-A}(\bar{c}_j b_i)_{V-A}, \quad Q_2 = (\bar{s}_i c_i)_{V-A}(\bar{c}_j b_j)_{V-A}, \\ Q_1^{\text{LR}} &= (\bar{s}_i c_j)_{V-A}(\bar{c}_j b_i)_{V+A}, \quad Q_2^{\text{LR}} = (\bar{s}_i c_i)_{V-A}(\bar{c}_j b_j)_{V+A}, \end{aligned} \tag{15}$$

and the Q_i^{RL} are chirality-flipped with respect to Q_i^{LR}. Operators of the type RR are not included into our analysis as their coefficients scale like v^4/M_{KK}^4 in the models at hand. Because of the hierarchies in the Cabibbo-Kobayashi-Maskawa (CKM) matrix and the RS-GIM mechanism, it is sufficient to restrict ourselves on c quarks as intermediate states, when we calculate the RS corrections involving the charged-current sector. For the SM contribution however, we include the combinations uc, cu, and uu in addition to the operators given above. Concerning the NP corrections LL, LR, RL, we pull out the CKM factor λ_c^{bs} for convenience. The measured values for V_{cb} and V_{cs}, extracted from semileptonic B and D decays, should be identified with the exchange of all $[SU(2)_L]$ W-type bosons. As a consequence, the NP coefficients $C_{1,2}^{\text{LL}}$ arise only due to nonfactorizable corrections, which can not be absorbed into λ_c^{bs}. We further have to include QCD penguin operators

$$\begin{aligned} Q_3 &= (\bar{s}_i b_i)_{V-A} \sum_q (\bar{q}_j q_j)_{V-A}, \\ Q_4 &= (\bar{s}_i b_j)_{V-A} \sum_q (\bar{q}_j q_i)_{V-A}, \\ Q_5 &= (\bar{s}_i b_i)_{V-A} \sum_q (\bar{q}_j q_j)_{V+A}, \\ Q_6 &= (\bar{s}_i b_j)_{V-A} \sum_q (\bar{q}_j q_i)_{V+A}, \end{aligned} \tag{16}$$

as well as EW penguin operators

$$\begin{aligned} Q_7 &= \frac{3}{2}(\bar{s}_i b_i)_{V-A} \sum_q Q_q (\bar{q}_j q_j)_{V+A}, \\ Q_8 &= \frac{3}{2}(\bar{s}_i b_j)_{V-A} \sum_q Q_q (\bar{q}_j q_i)_{V+A}, \\ Q_9 &= \frac{3}{2}(\bar{s}_i b_i)_{V-A} \sum_q Q_q (\bar{q}_j q_j)_{V-A}, \\ Q_{10} &= \frac{3}{2}(\bar{s}_i b_j)_{V-A} \sum_q Q_q (\bar{q}_j q_i)_{V-A}, \end{aligned} \tag{17}$$

where $q = u, c, d, s$, and Q_q is the electric charge. Here, no CKM factors are involved and one has to keep all light quarks as intermediate states if one considers neutral-current insertions only. The operators $\tilde{Q}_{3\ldots10}$ are chirality-flipped with respect to (16) and (17). In principle, there is the possibility of a flavor change on both vertices for NP penguins, and the Wilson coefficients depend on the quark flavor q. However, these effects suffer from an additional RS-GIM suppression and can be neglected for all practical purposes. For the same reason the chirality-flipped penguins $\tilde{C}_{3\ldots10}^{\text{RS}}$ can be neglected compared to $C_{3\ldots10}^{\text{RS}}$ for bs transitions [13]. Within the minimal RS model it will turn out that, despite of the α/α_s-suppression, the EW penguin operators can dominate over the gluon penguins [13–15]. This is explained by an extra factor L, which shows up in the leading correction to the left-handed Z^0-coupling. Note that this is not the case in the custodial RS variant [23,24], which features a protection for the $Zb_L\bar{b}_L$ vertex. The RS Wilson coefficients of the penguin operators can be found

in [13] and are collected in Appendix B for completeness. There further is the possibility of flavor-changing Higgs couplings which, however, can be neglected against the contributions of flavor-changing heavy gauge bosons in RS models.

Concerning the double-penguin insertions, we include all light quarks with masses set to zero (besides m_c). The double-penguin insertion also allows for leptons within the cut-diagram. However, as the related SM coefficient is suppressed by α/α_s, there is no chance to obtain big effects from $\bar{s}b \to \bar{\tau}\tau$ transitions, which are less constrained by experiment [33]. Note that this is not a general statement about NP models. If there is a tree-level transition $\bar{s}b \to \bar{\tau}\tau$ mediated by light NP particles in the range of $\sim$100 GeV, the double NP insertion becomes comparable to the SM diagrams [34]. Possible candidates are scalar leptoquarks [9,35]. Neglecting intermediate leptons, we find to LO in $1/m_b$

$$
\begin{aligned}
\Gamma_{12}^s = & -\frac{m_b^2}{12\pi(2M_{B_s})} G_F^2 (\lambda_c^{bs})^2 \sqrt{1-4z} \Bigg\{ \Bigg[(1-z)(\Sigma_1 + \Sigma_1^{\mathrm{LL}}) + \frac{1}{2}(1-4z)(\Sigma_2 + \Sigma_2^{\mathrm{LL}}) + 3z(\Sigma_3 + K_3'^{\mathrm{LL}}) \\
& - \frac{3}{2}\sqrt{z}(\Sigma_1^{\mathrm{LR}} + \Sigma_2^{\mathrm{LR}} + K_3'^{\mathrm{LR}} + K_4'^{\mathrm{LR}}) + \frac{1}{\sqrt{1-4z}} \Bigg((3\bar{K}_1'' + K_{s1}'' + \frac{3}{2}\bar{K}_2'' + \frac{1}{2}K_{s2}'') + \frac{\lambda_u^{bs}}{\lambda_c^{bs}}(1-z)^2((2+z)K_1 \\
& + (1-z)K_2) + \frac{1}{2}\frac{(\lambda_u^{bs})^2}{(\lambda_c^{bs})^2}(2K_1 + K_2) \Bigg) \Bigg] \langle \mathcal{Q}_1 \rangle + \Bigg[(1+2z)(\Sigma_1 + \Sigma_1^{\mathrm{LL}} - \Sigma_2 - \Sigma_2^{\mathrm{LL}}) - 3\sqrt{z}(2\Sigma_1^{\mathrm{LR}} + \Sigma_2^{\mathrm{LR}} - K_4'^{\mathrm{LR}}) \\
& + \frac{1}{\sqrt{1-4z}} \Bigg((3\bar{K}_1'' + K_{s1}'' - 3\bar{K}_2'' - K_{s2}'') + 2\frac{\lambda_u^{bs}}{\lambda_c^{bs}}(1-z)^2(1+2z)(K_1 - K_2) + \frac{(\lambda_u^{bs})^2}{(\lambda_c^{bs})^2}(K_1 - K_2) \Bigg) \Bigg] \langle \mathcal{Q}_2 \rangle \\
& - 3\sqrt{z}(\Sigma_1^{\mathrm{LR}} + 2\Sigma_2^{\mathrm{LR}} + K_3'^{\mathrm{LR}}) \langle \mathcal{Q}_3 \rangle + 3\sqrt{z}(\Sigma_1^{\mathrm{RL}} - K_3'^{\mathrm{RL}}) \langle \mathcal{Q}_4 \rangle + 3\sqrt{z}(\Sigma_2^{\mathrm{RL}} - K_4'^{\mathrm{RL}}) \langle \mathcal{Q}_5 \rangle \Bigg\} \\
& - \frac{m_b^2}{12\pi(2M_{B_s})} \sqrt{2} G_F \lambda_c^{bs} \sqrt{1-4z} \Bigg\{ \Bigg[(1-z)\Sigma_1^{\mathrm{NP}} + \frac{1}{2}(1-4z)\Sigma_2^{\mathrm{NP}} + 3z\Sigma_3^{\mathrm{NP}} \\
& + \frac{1}{\sqrt{1-4z}} \Bigg(3\bar{K}_1'^{\mathrm{NP}} + K_{s1}'^{\mathrm{NP}} + \frac{3}{2}\bar{K}_2'^{\mathrm{NP}} + \frac{1}{2}K_{s2}'^{\mathrm{NP}} \Bigg) \Bigg] \langle \mathcal{Q}_1 \rangle + \Bigg[(1+2z)(\Sigma_1^{\mathrm{NP}} - \Sigma_2^{\mathrm{NP}}) \\
& + \frac{1}{\sqrt{1-4z}} (3\bar{K}_1'^{\mathrm{NP}} + K_{s1}'^{\mathrm{NP}} - 3\bar{K}_2'^{\mathrm{NP}} - K_{s2}'^{\mathrm{NP}}) \Bigg] \langle \mathcal{Q}_2 \rangle + \mathcal{O}\left(\frac{1}{m_b}\right) \Bigg\},
\end{aligned}
\tag{18}
$$

where $z = m_c^2/m_b^2$ and $\langle \mathcal{Q} \rangle \equiv \langle B_s^0 | \mathcal{Q} | \bar{B}_s^0 \rangle$. In order to get a compact result, we have defined the linear combinations (A, B $\in$ {L, R})

$$
\begin{aligned}
\Sigma_i &= K_i + K_i' + K_i'', \qquad \Sigma_i^{\mathrm{AB}} = K_i^{\mathrm{AB}} + K_i'^{\mathrm{AB}}, \qquad i = 1, 2, \\
\Sigma_3 &= K_3' + K_3'', \qquad \Sigma_i^{\mathrm{NP}} = K_i'^{\mathrm{NP}} + K_i''^{\mathrm{NP}} \qquad i = 1, 2, 3,
\end{aligned}
\tag{19}
$$

where the coefficients on the right-hand side of (19) are themselves linear combinations of Wilson coefficients. In agreement with [27] we have ($C_{i+j} \equiv C_i + C_j$)

$$
\begin{aligned}
& K_1 = N_c C_1^2 + 2C_1 C_2, \qquad K_2 = C_2^2, \qquad K_1' = 2(N_c C_1 C_{3+9} + C_1 C_{4+10} + C_2 C_{3+9}), \qquad K_2' = 2C_2 C_{4+10}, \\
& K_3' = 2(N_c C_1 C_{5+7} + C_1 C_{6+8} + C_2 C_{5+7} + C_2 C_{6+8}), \qquad K_1'' = N_c C_{3+9}^2 + 2C_{3+9} C_{4+10} + N_c C_{5+7}^2 + 2C_{5+7} C_{6+8}, \\
& K_2'' = C_{4+10}^2 + C_{6+8}^2, \qquad K_3'' = 2(N_c C_{3+9} C_{5+7} + C_{3+9} C_{6+8} + C_{4+10} C_{5+7} + C_{4+10} C_{6+8}).
\end{aligned}
\tag{20}
$$

The combinations K_i stem from the insertion of charged-current operators and give the dominant contribution in the SM. The coefficients K_i' and K_i'' correspond to the interference of charged-current with penguin operators and penguin-penguin insertions, respectively. As we consider light quarks ($q = u, d, s$) in the limit $m_q = 0$, there is a cancellation in the EW penguin sector due to the electric charges. The coefficients $\bar{K}_i''$ therefore resemble the K_i'', with $C_{7\ldots10}$ set to zero. For strange quarks as intermediate states, there is a second possibility for the penguin insertion. In the limit $m_s = 0$, there are additional contributions

$$
\begin{aligned}
K_{s1}'' &= (2+N_c)(C_4 - C_{10}/2)^2 + 2(N_c+1)(C_3 - C_9/2) \\
&\quad \times (C_4 - C_{10}/2) + 2(C_3 - C_9/2)^2, \\
K_{s2}'' &= 2(C_3 - C_9/2)(C_4 - C_{10}/2) + (C_3 - C_9/2)^2.
\end{aligned}
\tag{21}
$$

Note that these terms have not been taken into account in [27]. However, as all double-penguin insertions are numerically suppressed, this omission has no significant

effect. Next we come to the interference of SM diagrams with NP penguins, which is collected in

$$\begin{aligned}
K_1'^{\rm NP} &= 2(N_c C_1 C_{3+9}^{\rm NP} + C_1 C_{4+10}^{\rm NP} + C_2 C_{3+9}^{\rm NP}),\\
K_2'^{\rm NP} &= 2C_2 C_{4+10}^{\rm NP},\\
K_3'^{\rm NP} &= 2(N_c C_1 C_{5+7}^{\rm NP} + C_1 C_{6+8}^{\rm NP} + C_2 C_{5+7}^{\rm NP} + C_2 C_{6+8}^{\rm NP}),\\
K_{s1}''^{\rm NP} &= 2((N_c+2)C_4(C_4^{\rm NP} - C_{10}^{\rm NP}/2)\\
&\quad + (N_c+1)C_4(C_3^{\rm NP} - C_9^{\rm NP}/2)\\
&\quad + (N_c+1)C_3(C_4^{\rm NP} - C_{10}^{\rm NP}/2) + 2C_3(C_3^{\rm NP} - C_9^{\rm NP}/2)),\\
K_{s2}''^{\rm NP} &= 2(C_3(C_3^{\rm NP} - C_9^{\rm NP}/2) + C_3(C_4^{\rm NP} - C_{10}^{\rm NP}/2)\\
&\quad + C_4(C_3^{\rm NP} - C_9^{\rm NP}/2))
\end{aligned} \tag{22}$$

and

$$\begin{aligned}
K_1''^{\rm NP} &= 2(N_c C_3 C_{3+9}^{\rm NP} + C_3 C_{4+10}^{\rm NP} + C_4 C_{3+9}^{\rm NP} + N_c C_5 C_{5+7}^{\rm NP}\\
&\quad + C_5 C_{6+8}^{\rm NP} + C_6 C_{5+7}^{\rm NP}),\\
K_2''^{\rm NP} &= 2(C_4 C_{4+10}^{\rm NP} + C_6 C_{6+8}^{\rm NP}),\\
K_3''^{\rm NP} &= 2(N_c C_3 C_{5+7}^{\rm NP} + C_3 C_{6+8}^{\rm NP} + C_4 C_{5+7}^{\rm NP} + C_4 C_{6+8}^{\rm NP}\\
&\quad + N_c C_5 C_{3+9}^{\rm NP} + C_5 C_{4+10}^{\rm NP} + C_6 C_{3+9}^{\rm NP} + C_6 C_{4+10}^{\rm NP}).
\end{aligned} \tag{23}$$

Here, we have neglected the tiny contributions from the interference of SM EW penguins with NP graphs. There further is interference between NP charged currents and SM penguins

$$\begin{aligned}
K_1'^{\rm LL} &= 2(N_c C_3 C_1^{\rm LL} + C_3 C_2^{\rm LL} + C_4 C_1^{\rm LL}),\\
K_2'^{\rm LL} &= 2C_4 C_2^{\rm LL},\\
K_3'^{\rm LL} &= 2(N_c C_5 C_1^{\rm LL} + C_5 C_2^{\rm LL} + C_6 C_1^{\rm LL} + C_6 C_2^{\rm LL}),\\
K_1'^{\rm LR} &= 2(N_c C_3 C_1^{\rm LR} + C_3 C_2^{\rm LR} + C_4 C_1^{\rm LR}),\\
K_2'^{\rm LR} &= 2C_4 C_2^{\rm LR},\\
K_3'^{\rm LR} &= 2(N_c C_5 C_1^{\rm LR} + C_5 C_2^{\rm LR} + C_6 C_1^{\rm LR}),\\
K_4'^{\rm LR} &= 2C_6 C_2^{\rm LR}.
\end{aligned} \tag{24}$$

The corrections to the purely charged-current interactions are collected into

$$\begin{aligned}
K_1^{\rm LL} &= 2(N_c C_1 C_1^{\rm LL} + C_1 C_2^{\rm LL} + C_2 C_1^{\rm LL}),\\
K_2^{\rm LL} &= 2C_2 C_2^{\rm LL},\\
K_1^{\rm LR} &= 2(N_c C_1 C_1^{\rm LR} + C_1 C_2^{\rm LR} + C_2 C_1^{\rm LR}),\\
K_2^{\rm LR} &= 2C_2 C_2^{\rm LR}.
\end{aligned} \tag{25}$$

The coefficients $K_i^{(\prime)\rm RL}$ resemble $K_i^{(\prime)\rm LR}$, with $C_i^{\rm LR}$ replaced by $C_i^{\rm RL}$. All NP coefficients should by calculated at the NP mass scale and then be evolved down to m_b. Explicit expressions for the minimal and the custodial RS model can be found in the appendixes.

For the sake of completeness, we finally quote the known results for the mixing amplitude. One defines

$$\mathcal{H}_{\rm eff}^{\Delta B=2} = \sum_{i=1}^{5} C_i \mathcal{Q}_i + \sum_{i=1}^{3} \tilde{C}_i \tilde{\mathcal{Q}}_i, \tag{26}$$

where there are no tree-level contributions to $C_{2,3}$ and $\tilde{C}_{2,3}$ in the RS model [12,13]. The RS correction to

$$2m_{B_s} M_{12}^s = \langle B_s^0 | \mathcal{H}_{\rm eff}^{\Delta B=2} | \bar{B}_s^0 \rangle \tag{27}$$

can be found in [12,13], and is given by

$$\begin{aligned}
M_{12}^{s\rm RS} &= \frac{4}{3} m_{B_s} f_{B_s}^2 \Big[(C_1^{\rm RS}(\bar{m}_b) + \tilde{C}_1^{\rm RS}(\bar{m}_b)) B_1\\
&\quad + \frac{3}{4} R(\bar{m}_b) C_4^{\rm RS}(\bar{m}_b) B_4 + \frac{1}{4} R(\bar{m}_b) C_5^{\rm RS}(\bar{m}_b) B_5 \Big].
\end{aligned} \tag{28}$$

The bag parameters $B_{1,4,5}$ are listed in (34), and the $\Delta B = 2$ coefficients can be found in Appendix C. Compared to $C_1^{\rm RS}(\bar{m}_b)$, the coefficient $C_4^{\rm RS}(\bar{m}_b)$ is suppressed by about 2 orders of magnitude due to a stronger RS-GIM mechanism. The coefficients $\tilde{C}_1^{\rm RS}(\bar{m}_b)$ and $C_5^{\rm RS}(\bar{m}_b)$ are even further suppressed. The SM mixing amplitude can be taken from [3,36,37]

$$M_{12}^{s\rm SM} = \frac{G_F^2}{12\pi^2} (\lambda_t^{bs})^2 m_W^2 m_{B_s} \eta_B f_{B_s}^2 B_1 S_0(x_t), \tag{29}$$

where $\eta_B = 0.837$ involves NLO QCD corrections in naive dimensional reduction (NDR). $S_0(x_t)$ is the Inami-Lim function and $x_t = \bar{m}_t(\bar{m}_t)^2/m_W^2$ with $\bar{m}_t(\bar{m}_t) = (163.8 \pm 2.0)$ GeV. The meson mass and decay constant are given by $m_{B_s} = 5.366(1)$ GeV [38] and $f_{B_s} = (238.8 \pm 9.5)$ MeV [39], respectively. If not stated otherwise, all other experimental input is taken from [38].

IV. NUMERICAL ANALYSIS

In order to obtain the RS predictions, we need an appropriate set of input parameters, consisting of the Yukawa matrices, the bulk-mass parameters c_{Q_i} and c_{q_i} of the $SU(2)_L$-doublet and singlet fermions, as well as the KK scale $M_{\rm KK}$. Within an anarchic approach to flavor, all Yukawa entries are chosen to be of $\mathcal{O}(1)$. The generation of input points is most easily achieved by making use of the warped-space Froggatt-Nielsen mechanism [15,17], which provides simple analytic expressions for the fermion masses and Wolfenstein parameters in terms of the zero-mode profiles (9) and entries of the Yukawa matrices, but independent of $M_{\rm KK}$ to first approximation. In our analysis, we use 10 000 randomly generated parameter sets with $|(Y_{u,d})_{ij}| \in [0.1, 3]$, which guarantees perturbativity of the Yukawa couplings in higher order corrections [40]. The points are chosen such that they fit the correct

zero-mode masses, CKM mixing angles and phase in standard convention [38] within the 1σ range.

The contributions of some individual ingredients of Γ_{12}^s (18) are summarized in Table I. The SM coefficients are taken from [41]. For the sake of comparison, we rescale the RS penguin coefficients, for instance $\tilde{K}_2^{\prime\mathrm{RS}} \equiv \sqrt{2}(G_F\lambda_c^{bs})^{-1}K_2^{\prime\mathrm{RS}}$ (SM: $\tilde{K}_2^{\prime} = K_2^{\prime}$), as they are not supplemented with a CKM factor in (14). We compare the mean absolute values of our RS predictions to the corresponding sizes of the SM coefficients, where the numbers have to be multiplied by the order of magnitude given in the last column of Table I. The maximum values exceed the given numbers by at least 1 order of magnitude, as suggested by the large standard deviations. The NP mass scale is set to $M_{\mathrm{KK}} = 2$ TeV and we discard all points, which are in conflict with the $Z^0 \to b\bar{b}$ "pseudo observables." These are the ratio of the width of the Z^0-boson decay into bottom quarks and the total hadronic width, R_b^0, the bottom quark left-right asymmetry parameter A_b, and the forward-backward asymmetry for bottom quarks $A_{\mathrm{FB}}^{0,b}$, which set an upper limit on $c_{b_L} \equiv c_{Q_3}$ [17]. For $M_{\mathrm{KK}} = 2$ TeV, most of the points with $c_{b_L} > -0.5$ are excluded. On the other hand, for $\mathcal{O}(1)$ Yukawa couplings, the top-quark mass only allows for a minimal UV localization of the $(t_L, b_L)^T$ doublet. Thus, the valid bulk-mass parameters c_{Q_3} are clustered around $-1/2$. We reject all points which lie outside the 95% confidence region in the $g_L^b - g_R^b$ plane (see analysis in [17]). Within the custodial RS variant with protection of the $Z^0 b_L \bar{b}_L$-vertex, the related upper bound on c_{b_L} vanishes. On the other hand, there is no stringent upper bound on the bulk-mass parameter $c_{t_R} \equiv c_{u_3}$, which we allow to vary within $[-0.5, 1]$.

Neglecting experimental constraints, there is no difference between the minimal and the custodial RS variant at LO in v^2/M_{KK}^2 in the charged-current sector (see Appendix A). For the natural assumption of $c_{Q_2} < -1/2$ the biggest correction comes from the operator Q_2^{LR}. This is easy to understand if we apply the Froggatt-Nielsen analysis of [17] to (A5) and (A8). Setting all Yukawa factors to one, we can derive simple expressions for the Wilsons coefficients by performing an expansion in the Wolfenstein parameter $\lambda \approx 0.225$, which is related to ratios of IR zero-mode profiles [17]

$$\frac{|F(c_{Q_1})|}{|F(c_{Q_2})|} \sim \lambda, \qquad \frac{|F(c_{Q_2})|}{|F(c_{Q_3})|} \sim \lambda^2, \qquad |F(c_{Q_3})| \sim \mathcal{O}(1). \tag{30}$$

Thus, we find as a crude approximation

$$\begin{aligned} C_2^{\mathrm{LL}} &\propto \frac{m_W^2}{2M_{\mathrm{KK}}^2} L F(c_{Q_2})^2 F(c_{Q_3})^2, \\ C_2^{\mathrm{LR}} &\propto \frac{v^2}{2M_{\mathrm{KK}}^2} \frac{F(c_{Q_3})}{F(c_{Q_2})} F(c_{u_2}) F(c_{d_3}) \propto \frac{m_c m_b}{M_{\mathrm{KK}}^2} \frac{1}{F(c_{Q_2})^2}, \\ C_2^{\mathrm{RL}} &\propto \frac{v^2}{M_{\mathrm{KK}}^2} F(c_{u_2}) F(c_{d_2}) \propto \frac{2m_c m_s}{M_{\mathrm{KK}}^2} \frac{1}{F(c_{Q_2})^2}. \end{aligned} \tag{31}$$

Note that the importance of C_2^{LR} grows with increasing UV localization of the $(c_L, s_L)^T$ doublet. The coefficients C_1^{AB} with $\mathrm{A, B} \in \{\mathrm{L, R}\}$ are zero at the matching scale, but generated through operator mixing when running down to $\mu = \bar{m}_b$. As it turns out, the values of $|K_1^{\mathrm{AB}}|$ are about a third of the respective values of $|K_2^{\mathrm{AB}}|$ at $\mu = \bar{m}_b$. In the RS model the contributions from the coefficients C_i^{LL} and C_i^{RL} can be neglected, just as those of the chirality-flipped penguins. The coefficients $K_i^{\prime\mathrm{RS}}$ and $K_i^{\prime\prime\mathrm{RS}}$ grow with an increasing value of c_{b_L} and $c_{s_L} \equiv c_{Q_2}$. The reason is that the RS corrections due to penguin operators are dominated by overlap integrals of left-handed fermions with intermediate KK-gauge bosons and mixing effects of the latter with Z^0. The relevant expressions are given in (B1). As KK modes are peaked toward the IR-brane, overlap integrals with UV-localized fermions are exponentially suppressed and RS-GIM is at work. The leading correction due to Z^0 exchange is enhanced by a factor L within the minimal RS variant. Nevertheless, due to the stringent bounds from $Z^0 b\bar{b}$, the total penguin contributions remain smaller than in the custodial model. In both models, it is sufficient to consider just the contributions stemming from the coefficients K_i^{NP} in the neutral-current sector. The impact of double penguins is typically about 1% of the leading correction due to charged currents.

In order to get the overall picture, we have to evaluate the whole expressions (18) and (28). In terms of

$$R(\mu) \equiv \left(\frac{M_{B_s}}{\bar{m}_b(\mu) + \bar{m}_s(\mu)}\right)^2, \tag{32}$$

TABLE I. Selected SM penguin and charged-current coefficients contributing to Γ_{12}^s compared to the mean absolute values of the corresponding RS coefficients for $M_{\mathrm{KK}} = 2$ TeV and $\mu = \bar{m}_b$. See text for details.

Model/Coefficient	$\lvert\tilde{K}_2^{\prime}\rvert$	$\lvert\tilde{K}_2^{\prime\prime}\rvert$	$\lvert K_2^{(\mathrm{LL})}\rvert$	$\lvert K_2^{\mathrm{LR}}\rvert$	$\lvert K_2^{\mathrm{RL}}\rvert$	$\times$
SM	0.543	0.016	12.656			10^{-1}
Mean (minimal RS)	0.16	0.03	0.01	4.40	0.04	10^{-3}
Standard deviation	0.17	0.03	0.05	7.41	0.06	10^{-3}
Mean (custodial RS)	0.94	0.06	0.23	2.22	0.03	10^{-3}
Standard deviation	1.39	0.09	1.38	4.98	0.05	10^{-3}

the matrix elements are given by

$$\begin{aligned}\langle Q_1\rangle &= \frac{8}{3}M_{B_s}^2 f_{B_s}^2 B_1(\mu),\\ \langle Q_2\rangle &= -\frac{5}{3}M_{B_s}^2 f_{B_s}^2 R(\mu) B_2(\mu),\\ \langle Q_3\rangle &= \frac{1}{3}M_{B_s}^2 f_{B_s}^2 R(\mu) B_3(\mu),\\ \langle Q_4\rangle &= 2M_{B_s}^2 f_{B_s}^2 R(\mu) B_4(\mu),\\ \langle Q_5\rangle &= \frac{2}{3}M_{B_s}^2 f_{B_s}^2 R(\mu) B_5(\mu).\end{aligned} \tag{33}$$

The bag parameters B_i can be extracted from the lattice. We take the values of [42] in the NDR-$\overline{\text{MS}}$ scheme of [28]. They read

$$\begin{aligned} B_1 &= 0.87(2)\binom{+5}{-4}, \qquad B_2 = 0.84(2)(4),\\ B_3 &= 0.91(3)(8), \qquad B_4 = 1.16(2)\binom{+5}{-7},\\ B_5 &= 1.75(3)\binom{+21}{-6}, \end{aligned} \tag{34}$$

where the first (second) number in brackets corresponds to the statistical (systematic) error. In order to resum large logarithms we employ $\bar{z} = \bar{m}_c^2(\bar{m}_b)/\bar{m}_b^2(\bar{m}_b) = 0.048(4)$ [3] in our numerical analysis. We further use $\bar{m}_b(\bar{m}_b) = (4.22 \pm 0.08)$ GeV and $\bar{m}_s(\bar{m}_b) = (0.085 \pm 0.017)$ GeV.

In the first panel of Fig. 1 we show the RS corrections to the magnitude and CP-violating phase of the $\bar{B}_s^0$-B_s^0 decay width, R_Γ and ϕ_Γ, for a set of 10 000 parameter points for $M_{\text{KK}} = 2$ TeV. The blue (dark gray) points correspond to the minimal RS model, where we plot only those that are in agreement with the $Z^0 \to b\bar{b}$ pseudo observables. The orange (light gray) points correspond to the custodial extension, where the latter bound vanishes. As we are just interested in the approximate size of RS corrections, we work with the LO SM expressions. For precise predictions for a certain parameter point, one should include the full NLO corrections to Γ_{12}^s and M_{12}^s. As expected, the RS corrections to $|\Gamma_{12}^s|$ are rather small, typically not exceeding $\pm 4\%$. The corrections to the magnitude and phase of the dispersive part of the mixing amplitude, R_M and ϕ_M, are plotted in the second panel of Fig. 1. At this point, one should keep in mind the experimental result from the measurement of the $\bar{B}_s^0$-B_s^0 oscillation frequency [43]

$$\Delta m_{B_s}^{\text{exp}} = (17.77 \pm 0.10\,(\text{stat}) \pm 0.07\,(\text{syst}))\ \text{ps}^{-1}, \tag{35}$$

which is in good agreement with the SM prediction (17.3 ± 2.6) ps^{-1} [10]. As a consequence, all points with $R_M \notin [0.718, 1.336]$ are excluded at 95% confidence level, as indicated by the dashed lines. For a sufficient amount of scatter points, the phase correction ϕ_M can take any value of $[-\pi, \pi]$ within the custodial RS model. Compared to

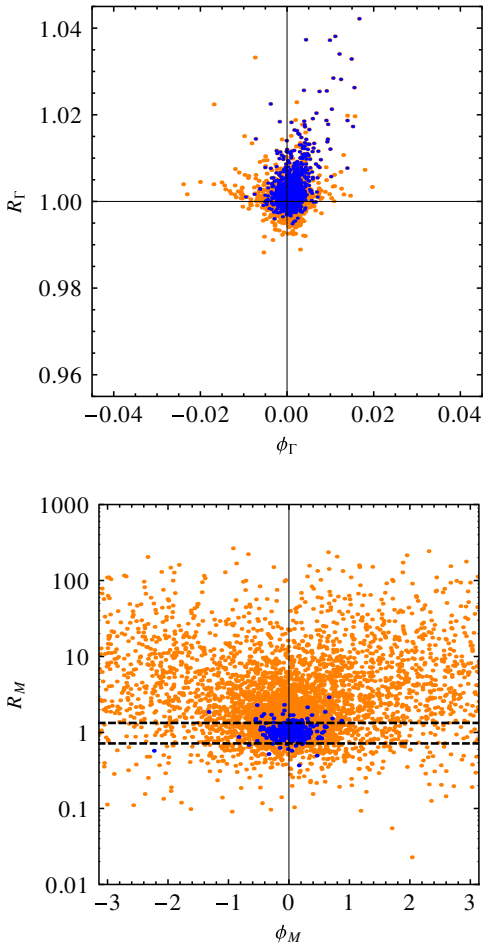

FIG. 1 (color online). RS corrections to the magnitude and CP-violating phase of the $\bar{B}_s^0$-B_s^0 decay amplitude, R_Γ and ϕ_Γ, as well as for the mixing amplitude, R_M and ϕ_M. Blue (dark gray) points correspond to the minimal, orange (light gray) to the custodial RS model. The dashed lines mark the 95% confidence region with respect to the measurement of Δm_{B_s}. See text for details.

ϕ_M, the new phase ϕ_Γ can be neglected (what we will do from now on).

We further take into account additional constraints from $\epsilon_K = \epsilon_K^{\text{SM}} + \epsilon_K^{\text{RS}}$ [12,13,40,44,45]. Explicitly, one needs to satisfy $|\epsilon_K| \in [1.2, 3.2] \times 10^{-3}$, where

$$\epsilon_K = \frac{\kappa_\epsilon e^{i\varphi_\epsilon}}{\sqrt{2}(\Delta m_K)_{\text{exp}}}\,\text{Im}(M_{12}^{K\text{SM}} + M_{12}^{K\text{RS}}), \tag{36}$$

with $\varphi_\epsilon = (43.51 \pm 0.05)^\circ$ [38] and $\kappa_\epsilon = 0.92 \pm 0.02$ [46]. The neutral kaon mixing amplitude is defined in analogy to (27). The input data needed for the calculation is given in Appendix B of [13]. As it turns out, without some tuning, the prediction for ϵ_K is generically too large. The dangerous contributions from the operators $Q_{4,5}^{sd}$ [40,44], which can become comparable to those of Q_1^{sd} due to $R_K = (M_K/(\bar{m}_d + \bar{m}_s))^2 \approx 20$ for $\mu = 2$ GeV and a more pronounced renormalization group running, can be

suppressed by imposing a $U(3)$ flavor symmetry in the right-handed down-quark sector. This symmetry is broken by the Yukawa couplings to obtain the correct zero-mode masses [47]. Nevertheless, if all bulk masses are equal, there are no tree-level FCNCs in the ZMA. This is evident from (C1), as $(\boldsymbol{W}_d^\dagger)_{mj}(\boldsymbol{W}_d)_{jn} = 0$ for $m \neq n$ due to the unitarity of $\boldsymbol{W}_d$. Nonvanishing contributions from the exchange of KK-gauge bosons arise from the mixing of the right-handed fermion zero modes with their KK excitations, thus involving an additional v^2/M_{KK}^2-suppression factor. For $M_{\mathrm{KK}} = 2$ TeV, one could therefore reduce $C_{4,5}^{sd}$ by a factor of about 100. The same suppression factor then applies to the B-meson sector. For the coefficient C_1^{RS}, there is no such protection. In our analysis, however, we do not impose an additional flavor symmetry on the bulk masses, but rather use the bound from ϵ_K as a filter for our scattering points.

Neglecting the small SM phases, the width difference (5) can be written as

$$\Delta\Gamma_s = \Delta\Gamma_s^{\mathrm{SM}} R_\Gamma \cos 2\beta_s, \tag{37}$$

where $2\beta_s \approx -\phi_M^{\mathrm{RS}}$ [4]. The preliminary CDF analysis [5] uses the older SM prediction $\Delta\Gamma_s^{\mathrm{SM}} = (0.096 \pm 0.039)\ \mathrm{ps}^{-1}$ [3], which we will take as central value for our calculation. Taking the more recent value will not change our conclusions. The resulting RS predictions for $\Delta\Gamma_s$ are plotted against β_s in the upper panel of Fig. 2. Comparing to the CDF results in the lower panel, we conclude that the RS model can enter the 68% confidence region and come close to the best-fit value. It stays below the desired value for $\Delta\Gamma_s$, as there are no sizable positive corrections to $|\Gamma_{12}^s|$.

It should be noted that the latest LHCb result for the phase $\phi_s^{J/\psi\phi} = -2\beta_s^{J/\psi\phi} = 0.03 \pm 0.16 \pm 0.07$ agrees with the SM prediction (3) within errors. The above number combines measurements of B_s^0 decays into $J/\psi\phi$ and $J/\psi f_0$ [48,49]. In agreement with the Tevatron results, an enhancement of the width difference compared to the SM value has been found. The best-fit value is given by $\Delta\Gamma_s = (0.123 \pm 0.029 \pm 0.011)\ \mathrm{ps}^{-1}$ [48].

The SM prediction $(A_{\mathrm{SL}}^s)_{\mathrm{SM}} = (1.9 \pm 0.3) \times 10^{-5}$ [10], which is often named a_{sl}^s or a_{fs}^s in the literature, agrees with the direct measurement $(A_{\mathrm{SL}}^s)_{\mathrm{exp}} = -0.0017 \pm 0.0092$ [50] within the (large) error. However, recent measurements of the like-sign dimuon charge asymmetry A_{SL}^b [51], which connects A_{SL}^s to its counterpart A_{SL}^d of the B_d^0-meson sector [52], imply a deviation of almost 2σ. If one neglects the tiny SM phases and the NP phase corrections related to decay, A_{SL}^s is proportional to the quantity $S_{\psi\phi}$ [6], which is given by the amplitude of the time-dependent asymmetry in $B_s^0 \to J/\psi\phi$ decays, $A_{CP}^s(t) = S_{\psi\phi} \sin(\Delta m_{B_s} t)$. Setting just the NP phase in decay to zero, one obtains the well-known expression $S_{\psi\phi} = \sin(2\beta_s^{J/\psi\phi} - \phi_M)$ [53], and thus

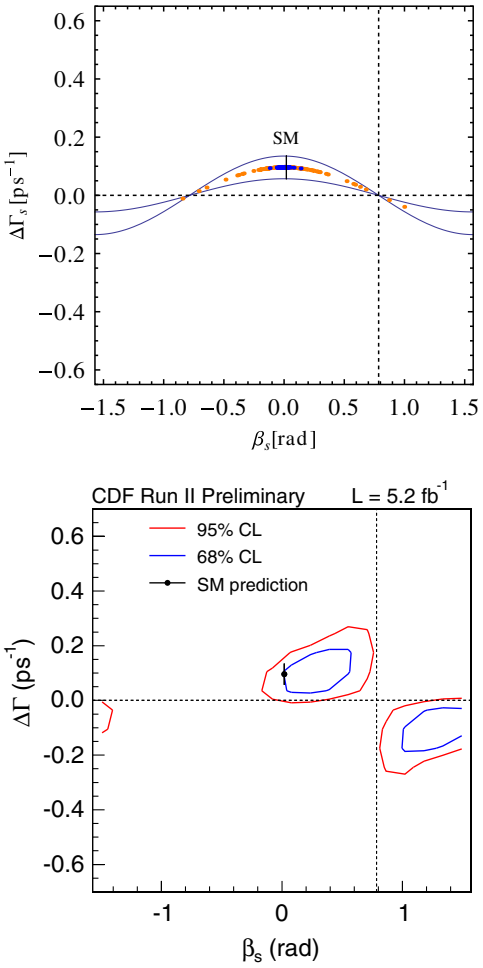

FIG. 2 (color online). Upper panel: Corrections within the $\Delta\Gamma_s^{\mathrm{SM}}/\beta_s$-plane for the minimal (blue/dark gray) and custodial (orange/light gray) RS model. Bounds from $Z^0 b\bar{b}$, Δm_{B_s}, and ϵ_K are satisfied. See text for details. Lower panel: Experimental constraints from flavor-tagged $B_s^0 \to J/\psi\phi$ decays. Figure taken from [5].

$$A_{\mathrm{SL}}^s \approx -\frac{|\Gamma_{12}^{s\mathrm{SM}}|}{|M_{12}^{s\mathrm{SM}}|}\frac{R_\Gamma}{R_M} S_{\psi\phi}. \tag{38}$$

The RS result is shown in Fig. 3, where we have sketched the experimental favored values $S_{\psi\phi} = 0.56 \pm 0.22$ [54] and $A_{\mathrm{SL}}^s = -0.0085 \pm 0.0058$ [50]. The latter number combines the direct measurement with the results derived from the measurement of A_{SL}^b in semileptonic B-decays together with the average $A_{\mathrm{SL}}^d = -0.0047 \pm 0.0046$ from B-factories. It is evident from the plot that the best-fit value of $S_{\psi\phi}$ can be reproduced (with some tuning in the minimal RS variant), which has already been noted in [12,13]. Furthermore, the custodial RS model can enter the 1σ range of the measured value of A_{SL}^s. The same conclusion has been drawn in [16] recently, using a different approach. Here, the authors did not produce any concrete sets of input

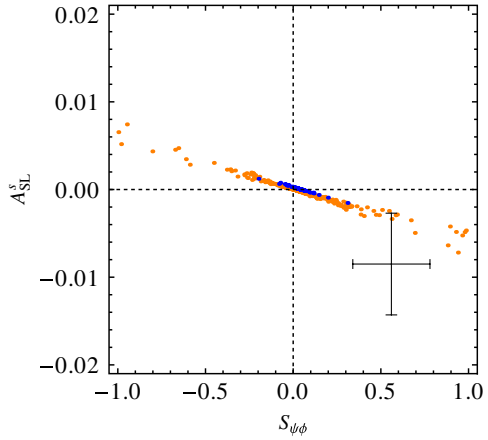

FIG. 3 (color online). Corrections within the $A^s_{\rm SL}/S_{\psi\phi}$-plane for the minimal (blue/dark gray) and custodial (orange/light gray) RS model. Bounds from $Z^0 b\bar{b}$, Δm_{B_s}, and ϵ_K are satisfied. See text for details.

parameters, but scanned FCNC vertices across the allowed range subject to bounds from $\Delta\Gamma_s$ and Δm_{B_s}.

Note that due to $S_{\psi\phi} \approx \sin 2\beta_s$, the corrections in the $\Delta\Gamma^{\rm SM}_s/\beta_s$-plane and the $A^s_{\rm SL}/S_{\psi\phi}$-plane are correlated. An improvement in the former leads to an improvement in the latter.

V. CONCLUSIONS

In this paper, we investigated the impact of RS models on the width difference $\Delta\Gamma_s$ of the $\bar{B}^0_s$-B^0_s system and the related CP-violating observables $A^s_{\rm SL}$ and $S_{\psi\phi}$. Therefore we calculated the leading corrections to Γ^s_{12} in terms of NP Wilson coefficients and took the known analytic expression for M^s_{12}. As we use an effective Hamiltonian approach, our result for Γ^s_{12} can be applied to other NP models. Our analysis involves a scan over a set of 10 000 random points reproducing the correct low-energy spectrum as well as the CKM mixing angles and phase. Bounds from $Z^0 b\bar{b}$, ϵ_K, and Δm_{B_s} have been taken into account. Because of the protection of the $Z^0 b_L \bar{b}_L$ vertex, the custodial extension allows for bulk masses $c_{b_L} > -1/2$, which enlarges the contribution of RS penguin operators and LL charged currents. While corrections to the magnitude and phase of Γ^s_{12} turn out to be small, where for both RS variants the biggest contribution comes from $\mathcal{Q}^{\rm LR}_2$ for most of the allowed parameter space, the new CP-violating phase in M^s_{12} allows to relax the disagreement between theory and experiment. Concerning the combined $\Delta\Gamma_s/\beta_s$ analysis, it is possible to enter the 68% confidence region. In order to reach the best-fit value however, moderate corrections to $|\Gamma^s_{12}|$ would be required [9], which are unlikely to appear in the models at hand. For the case of the semileptonic CP asymmetry $A^s_{\rm SL}$, agreement can be obtained within 1σ, where, at the same time, the best-fit value of $S_{\psi\phi}$ can be reached.

ACKNOWLEDGMENTS

We thank Martin Bauer, Sandro Casagrande, Uli Haisch, Tobias Hurth, Matthias Neubert, and Uli Nierste for useful discussions and remarks.

APPENDIX A: WILSON COEFFICIENTS OF CHARGED-CURRENT OPERATORS

The effective four-quark charged-current Hamiltonian can be written as

$$\mathcal{H}^{(W)}_{\rm eff} = 2\sqrt{2}G_F\{[\bar{d}_{m_L}\gamma_\mu(\mathbf{V}^\dagger_L)_{mn}u_{n_L} + \bar{d}_{m_R}\gamma_\mu(\mathbf{V}^\dagger_R)_{mn}u_{n_R}] \otimes [\bar{u}_{m'_L}\gamma^\mu(\mathbf{V}_L)_{m'n'}d_{n'_L} + \bar{u}_{m'_R}\gamma^\mu(\mathbf{V}_R)_{m'n'}d_{n'_R}] (+\text{H.c.})\}, \tag{A1}$$

where $m, n, m', n' \in \{1, 2, 3\}$, and a summation over the repeated indices is understood. Here, we have already absorbed a universal correction factor $(1 + m^2_W/(2M^2_{\rm KK}) \times [1 - 1/(2L)])$ into the Fermi constant due to the normalization to muon decay, from which G_F is extracted [17]. The tensor symbol merely indicates that the full analytic result contains terms that cannot be separated into independent matrix products. This is due to the sum over W-gauge boson profiles, which in the minimal model reads

$$2\pi\sum_{n=0}\frac{\chi_n(t)\chi_n(t')}{m^2_n} = \frac{1}{m^2_W} + \frac{1}{2M^2_{\rm KK}}\left[L(t^2_< - t^2 - t'^2) + 1 - \frac{1}{2L}\right], \tag{A2}$$

where $t^2_< \equiv \min(t^2, t'^2)$ [17], and we dropped terms of $\mathcal{O}(v^4/M^4_{\rm KK})$. The term $\propto t^2_<$ prevents a factorization into separate vertex factors. Performing the overlap integrals with the corresponding fermion profiles and employing the ZMA gives the rather simple result

$$(\mathbf{V}^\dagger_L)_{mn} \otimes (\mathbf{V}_L)_{m'n'} = (\boldsymbol{U}^\dagger_d\boldsymbol{U}_u)_{mn}(\boldsymbol{U}^\dagger_u\boldsymbol{U}_d)_{m'n'}\left[1 + \mathcal{O}\left(\frac{v^2}{M^2_{\rm KK}}\right)\right] + \frac{m^2_W}{2M^2_{\rm KK}}L(\boldsymbol{U}^\dagger_d)_{mi}(\boldsymbol{U}_u)_{in}(\tilde{\boldsymbol{\Delta}}_{QQ})_{ij}(\boldsymbol{U}^\dagger_u)_{m'j}(\boldsymbol{U}_d)_{jn'} \tag{A3}$$

with the nonfactorizable correction [45]

$$(\tilde{\boldsymbol{\Delta}}_{QQ})_{ij} = \frac{F^2(c_{Q_i})}{3 + 2c_{Q_i}}\frac{3 + c_{Q_i} + c_{Q_j}}{2 + c_{Q_i} + c_{Q_j}}\frac{F^2(c_{Q_j})}{3 + 2c_{Q_j}}. \tag{A4}$$

For B^0_s-meson decays, the whole expression has to be evaluated for $(m = 2, n = 2, m' = 2, n' = 3)$. Here, the leading term in (A3), together with factorizable corrections of the form $v^2/M^2_{\rm KK}(\cdots)_{mn}\cdot(\cdots)_{m'n'}$ [26], should be

identified with λ_c^{bs}. Concerning the custodial RS model, one would find additional factorizable terms, which also will be absorbed into CKM-matrix elements. Thus, we find at LO in $v^2/M_{\rm KK}^2$

$$C_2^{\rm LL}(M_{\rm KK}) = \frac{m_W^2}{2M_{\rm KK}^2} L \times \frac{(\boldsymbol{U}_d^\dagger)_{2i}(\boldsymbol{U}_u)_{i2}}{(\boldsymbol{U}_d^\dagger \boldsymbol{U}_u)_{22}} (\tilde{\boldsymbol{\Delta}}_{QQ})_{ij} \times \frac{(\boldsymbol{U}_u^\dagger)_{2j}(\boldsymbol{U}_d)_{j3}}{(\boldsymbol{U}_u^\dagger \boldsymbol{U}_d)_{23}}, \tag{A5}$$

independent of the chosen scenario, and $C_1^{\rm LL}(M_{\rm KK}) = 0$. The biggest corrections are found for $c_{Q_{2,3}} > -1/2$. For the mixed-chirality currents we have

$$\begin{aligned}(\mathbf{V}_L^\dagger)_{mn} \otimes (\mathbf{V}_R)_{m'n'} &= \frac{1}{M_{\rm KK}^2} (\boldsymbol{U}_d^\dagger \boldsymbol{U}_u)_{mn} (\boldsymbol{m}_u \boldsymbol{U}_u^\dagger)_{m'j} f(c_{Q_j}) \times (\boldsymbol{U}_d \boldsymbol{m}_d)_{jn'}, \\ (\mathbf{V}_R^\dagger)_{mn} \otimes (\mathbf{V}_L)_{m'n'} &= \frac{1}{M_{\rm KK}^2} (\boldsymbol{m}_d \boldsymbol{U}_d^\dagger)_{mi} f(c_{Q_i}) (\boldsymbol{U}_u \boldsymbol{m}_u)_{in} \times (\boldsymbol{U}_u^\dagger \boldsymbol{U}_d)_{m'n'}. \end{aligned} \tag{A6}$$

Here, $\boldsymbol{m}_u$ and $\boldsymbol{m}_d$ are 3×3 diagonal matrices containing the SM-like quark masses, and

$$f(c) = \frac{1}{F^2(c)(1-2c)} - \frac{1}{1-2c} + \frac{F^2(c)}{(1+2c)^2} \times \left(\frac{1}{1-2c} - 1 + \frac{1}{3+2c} \right). \tag{A7}$$

Modifications due to the custodial model are of higher order. We find the general RS prediction $C_1^{\rm LR/RL} = 0$ and

$$\begin{aligned} C_2^{\rm LR} &= \frac{1}{M_{\rm KK}^2} \frac{(\boldsymbol{m}_u \boldsymbol{U}_u^\dagger)_{2i} f(c_{Q_i}) (\boldsymbol{U}_d \boldsymbol{m}_d)_{i3}}{(\boldsymbol{U}_u^\dagger \boldsymbol{U}_d)_{23}}, \\ C_2^{\rm RL} &= \frac{1}{M_{\rm KK}^2} \frac{(\boldsymbol{m}_d \boldsymbol{U}_d^\dagger)_{2i} f(c_{Q_i}) (\boldsymbol{U}_u \boldsymbol{m}_u)_{i2}}{(\boldsymbol{U}_d^\dagger \boldsymbol{U}_u)_{22}}, \end{aligned} \tag{A8}$$

where the coefficients should be matched at the KK scale. The evolution down to the bottom mass is treated in Appendix D.

APPENDIX B: WILSON COEFFICIENTS OF PENGUIN OPERATORS

At $\mathcal{O}(v^2/M_{\rm KK}^2)$ the Wilson coefficients of the penguin operators in Eq. (14) are explicitly given by [13]

$$\begin{aligned} C_3^{\rm RS} &= \frac{\pi \alpha_s}{M_{\rm KK}^2} \frac{(\boldsymbol{\Delta}_D')_{23}}{2N_c} - \frac{\pi \alpha}{6 s_w^2 c_w^2 M_{\rm KK}^2} (\boldsymbol{\Sigma}_D)_{23}, \\ C_4^{\rm RS} &= C_6^{\rm RS} = -\frac{\pi \alpha_s}{2M_{\rm KK}^2} (\boldsymbol{\Delta}_D')_{23}, \\ C_5^{\rm RS} &= \frac{\pi \alpha_s}{M_{\rm KK}^2} \frac{(\boldsymbol{\Delta}_D')_{23}}{2N_c}, \\ C_7^{\rm RS} &= \frac{2\pi \alpha}{9M_{\rm KK}^2} (\boldsymbol{\Delta}_D')_{23} - \frac{2\pi \alpha}{3 c_w^2 M_{\rm KK}^2} (\boldsymbol{\Sigma}_D)_{23}, \\ C_8^{\rm RS} &= C_{10}^{\rm RS} = 0, \\ C_9^{\rm RS} &= \frac{2\pi \alpha}{9M_{\rm KK}^2} (\boldsymbol{\Delta}_D')_{23} + \frac{2\pi \alpha}{3 s_w^2 M_{\rm KK}^2} (\boldsymbol{\Sigma}_D)_{23}, \end{aligned} \tag{B1}$$

where s_w (c_w) is the sine (cosine) of the Weinberg angle, and

$$\boldsymbol{\Sigma}_D \equiv \omega_Z^{d_L} L \left(\frac{1}{2} - \frac{s_w^2}{3} \right) \boldsymbol{\Delta}_D + \frac{M_{\rm KK}^2}{m_Z^2} \boldsymbol{\delta}_D. \tag{B2}$$

These results are to be evaluated at the KK scale and are valid for the minimal RS variant for $\omega_Z^{d_L} = 1$. In the custodial RS model with $P_{\rm LR}$-symmetry, one finds $\omega_Z^{d_L} = 0$ [26]. Exact analytic expressions for $\boldsymbol{\Delta}_D$, $\boldsymbol{\Delta}_D'$, and $\boldsymbol{\delta}_D$ can be found in [17]. However, as we only deal with light SM quarks in the initial and final state, it is convenient to apply the ZMA to the above expressions. Therefore we have to replace

$$\begin{aligned} \boldsymbol{\Delta}_D &\to \boldsymbol{U}_d^\dagger \, \mathrm{diag}\left[\frac{F^2(c_{Q_i})}{3+2c_{Q_i}} \right] \boldsymbol{U}_d, \\ \boldsymbol{\Delta}_D' &\to \boldsymbol{U}_d^\dagger \, \mathrm{diag}\left[\frac{5+2c_{Q_i}}{2(3+2c_{Q_i})^2} F^2(c_{Q_i}) \right] \boldsymbol{U}_d, \end{aligned} \tag{B3}$$

as well as

$$\boldsymbol{\delta}_D \to \frac{1}{M_{\rm KK}^2} \boldsymbol{m}_d \boldsymbol{W}_d^\dagger \times \mathrm{diag}\left[\frac{1}{1-2c_{d_i}} \left(\frac{1}{F^2(c_{d_i})} - 1 + \frac{F^2(c_{d_i})}{3+2c_{d_i}} \right) \right] \boldsymbol{W}_d \boldsymbol{m}_d. \tag{B4}$$

In the custodial model with extended $P_{\rm LR}$-symmetry, the term $\propto 1/F^2(c_{d_i})$ in $\boldsymbol{\delta}_D$ is zero [26]. All other expressions hold for both scenarios. The running of the penguin coefficients is also treated in Appendix D.

APPENDIX C: WILSON COEFFICIENTS FOR $\Delta B = 2$ OPERATORS

The $\Delta B = 2$ operators that contribute to the $\bar{B}_s^0$-B_s^0 mixing amplitude at tree-level are given by $\mathcal{Q}_1$, $\tilde{\mathcal{Q}}_1$, $\mathcal{Q}_4$, and $\mathcal{Q}_5$. There is no mixing between $\mathcal{Q}_1$ and $\tilde{\mathcal{Q}}_1$ under renormalization. The anomalous dimension for both cases is given by $\gamma^{(0)\rm VLL} = 6 - 6/N_c$ [55]. The operators $\mathcal{Q}_{4,5}$ mix under renormalization and the anomalous dimension

matrix can be taken from [55,56]. The running of the coefficients is described by the general formula (D1). Defining $\tilde{\mathbf{\Delta}}_{dd}$ and $\tilde{\mathbf{\Delta}}_{Qd}$ in analogy to (A4), the RS coefficients evaluated at the KK scale are given by [13]

$$\begin{aligned}
C_1^{\mathrm{RS}} &= \frac{\pi L}{M_{\mathrm{KK}}^2}(\boldsymbol{U}_d^\dagger)_{2i}(\boldsymbol{U}_d)_{i3}(\tilde{\mathbf{\Delta}}_{QQ})_{ij}(\boldsymbol{U}_d^\dagger)_{2j}(\boldsymbol{U}_d)_{j3} \\
&\quad\times\left[\frac{\alpha_s}{2}\left(1-\frac{1}{N_c}\right)+Q_d^2\alpha+(\omega_Z^{d_Ld_L})\frac{(T_3^d-s_w^2Q_d)^2\alpha}{s_w^2c_w^2}\right], \\
\tilde{C}_1^{\mathrm{RS}} &= \frac{\pi L}{M_{\mathrm{KK}}^2}(\boldsymbol{W}_d^\dagger)_{2i}(\boldsymbol{W}_d)_{i3}(\tilde{\mathbf{\Delta}}_{dd})_{ij}(\boldsymbol{W}_d^\dagger)_{2j}(\boldsymbol{W}_d)_{j3} \\
&\quad\times\left[\frac{\alpha_s}{2}\left(1-\frac{1}{N_c}\right)+Q_d^2\alpha+(\omega_Z^{d_Rd_R})\frac{(s_w^2Q_d)^2\alpha}{s_w^2c_w^2}\right], \\
C_4^{\mathrm{RS}} &= -2\alpha_s\frac{\pi L}{M_{\mathrm{KK}}^2}(\boldsymbol{U}_d^\dagger)_{2i}(\boldsymbol{U}_d)_{i3}(\tilde{\mathbf{\Delta}}_{Qd})_{ij}(\boldsymbol{W}_d^\dagger)_{2j}(\boldsymbol{W}_d)_{j3} \\
C_5^{\mathrm{RS}} &= \frac{\pi L}{M_{\mathrm{KK}}^2}(\boldsymbol{U}_d^\dagger)_{2i}(\boldsymbol{U}_d)_{i3}(\tilde{\mathbf{\Delta}}_{Qd})_{ij}(\boldsymbol{W}_d^\dagger)_{2j}(\boldsymbol{W}_d)_{j3} \\
&\quad\times\left[\frac{2\alpha_s}{N_c}-4Q_d^2\alpha+\omega_Z^{d_Ld_R}\frac{4s_w^2Q_d(T_3^d-s_w^2Q_d)\alpha}{s_w^2c_w^2}\right].
\end{aligned} \tag{C1}$$

Here we have introduced the correction factors $\omega_Z^{qq'}$, which are equal to 1 in the minimal RS model, and given by

$$\begin{aligned}
\omega_Z^{qq'} &= 1+\frac{1}{c_w^2-s_w^2}\left(\frac{s_w^2(T_L^{3q}-Q^q)-c_w^2T_R^{3q}}{T_L^{3q}-s_w^2Q^q}\right) \\
&\quad\times\left(\frac{s_w^2(T_L^{3q'}-Q^{q'})-c_w^2T_R^{3q'}}{T_L^{3q'}-s_w^2Q^{q'}}\right)
\end{aligned} \tag{C2}$$

in the custodial RS variant with P_{LR}-symmetry. Numerically we find $\omega_Z^{d_Ld_L}\approx 2.9$, $\omega_Z^{d_Rd_R}\approx 150.9$, and $\omega_Z^{d_Ld_R}\approx -15.7$. The quantum numbers T_R^{3q} can be found in [26], and $T_L^{3d_L}\equiv T_3^d$.

APPENDIX D: RUNNING OF THE $\Delta B = 1$ COEFFICIENTS

Concerning the evolution of the RS Wilson coefficients, we will restrict ourselves to the LO running in α_s. Within the operator basis $\vec{Q}=(Q_1,Q_2,Q_{3\ldots10})$, the anomalous dimension matrix $\gamma^{(0)}$, which is a function of N_c, n_f, n_u, and n_d (number of colors, flavors, up-, and down-type quarks), can be found in [57,58]. The running of the coefficients is given by

$$\vec{C}(m_b)=U^{(5)}(m_b,m_t)U^{(6)}(m_t,M_{\mathrm{KK}})\vec{C}(M_{\mathrm{KK}}), \tag{D1}$$

where

$$U^{(n_f)}(\mu_1,\mu_2)=\hat{V}\left(\left[\frac{\alpha_s^{(n_f)}(\mu_2)}{\alpha_s^{(n_f)}(\mu_1)}\right]^{\vec{\gamma}^{(0)}/2\beta_0(n_f)}\right)_D\hat{V}^{-1}. \tag{D2}$$

Here, $\hat{V}$ diagonalizes $\gamma^{(0)^T}$ via ${\gamma^{(0)}}_D=\hat{V}^{-1}\gamma^{(0)^T}\hat{V}$, and $\vec{\gamma}^{(0)}$ contains the entries of ${\gamma^{(0)}}_D$. The QCD beta function is given by $\beta_0(n_f)=(11N_c-2n_f)/3$, and we fix the running of $\alpha_s(\mu)$ at $\mu=m_t=171.2$ GeV and $\mu=M_{\mathrm{KK}}=2$ TeV. As it turns out, there is a mixing between Q_1 and Q_2 independent of n_f, n_u, and n_d. The evolution in the penguin sector gets a small admixture from charged currents. The operators $Q_1^{\mathrm{LR/RL}}$ and $Q_2^{\mathrm{LR/RL}}$ do not mix into the penguin sector. Their internal mixing is identical to that of the LL operators, and there is no mixing between charged currents of different chiralities. For the running of the LR/RL coefficients, we insert

$$\gamma^{(0)}=\begin{pmatrix}-\frac{6}{N_c} & 6\\ 6 & -\frac{6}{N_c}\end{pmatrix} \tag{D3}$$

into Eq. (D1), where this formula also holds for the LL coefficients separately.

[1] A. J. Buras, W. Slominski, and H. Steger, Nucl. Phys. **B245**, 369 (1984).
[2] I. Dunietz, Ann. Phys. (N.Y.) **184**, 350 (1988).
[3] A. Lenz and U. Nierste, J. High Energy Phys. 06 (2007) 072.
[4] T. Aaltonen *et al.* (CDF Collaboration), CDF Note No. CDF/PHYS/BOTTOM/CDFR/9787, 2009.
[5] CDF Collaboration, CDF Note No. CDF/ANAL/BOTTOM/PUBLIC/10206, 2010.
[6] Z. Ligeti, M. Papucci, and G. Perez, Phys. Rev. Lett. **97**, 101801 (2006).
[7] Y. Grossman, Phys. Lett. B **380**, 99 (1996).
[8] I. Dunietz, R. Fleischer, and U. Nierste, Phys. Rev. D **63**, 114015 (2001).
[9] A. Dighe, A. Kundu, and S. Nandi, Phys. Rev. D **82**, 031502 (2010).
[10] A. Lenz and U. Nierste, arXiv:1102.4274.
[11] L. Randall and R. Sundrum, Phys. Rev. Lett. **83**, 3370 (1999).
[12] M. Blanke, A. J. Buras, B. Duling, S. Gori, and A. Weiler, J. High Energy Phys. 03 (2009) 001.
[13] M. Bauer, S. Casagrande, U. Haisch, and M. Neubert, J. High Energy Phys. 09 (2010) 017.
[14] K. Agashe, G. Perez, and A. Soni, Phys. Rev. Lett. **93**, 201804 (2004).

[15] K. Agashe, G. Perez, and A. Soni, Phys. Rev. D **71**, 016002 (2005).
[16] A. Datta, M. Duraisamy, and S. Khalil, Phys. Rev. D **83**, 094501 (2011).
[17] S. Casagrande, F. Goertz, U. Haisch, M. Neubert, and T. Pfoh, J. High Energy Phys. 10 (2008) 094.
[18] Y. Grossman and M. Neubert, Phys. Lett. B **474**, 361 (2000).
[19] T. Gherghetta and A. Pomarol, Nucl. Phys. **B586**, 141 (2000).
[20] H. Davoudiasl, J. L. Hewett, and T. G. Rizzo, Phys. Lett. B **473**, 43 (2000).
[21] A. Pomarol, Phys. Lett. B **486**, 153 (2000).
[22] S. J. Huber and Q. Shafi, Phys. Lett. B **498**, 256 (2001).
[23] K. Agashe, A. Delgado, M. J. May, and R. Sundrum, J. High Energy Phys. 08 (2003) 050.
[24] K. Agashe, R. Contino, L. Da Rold, and A. Pomarol, Phys. Lett. B **641**, 62 (2006).
[25] M. E. Albrecht, M. Blanke, A. J. Buras, B. Duling, and K. Gemmler, J. High Energy Phys. 09 (2009) 064.
[26] S. Casagrande, F. Goertz, U. Haisch, M. Neubert, and T. Pfoh, J. High Energy Phys. 09 (2010) 014.
[27] M. Beneke, G. Buchalla, and I. Dunietz, Phys. Rev. D **54**, 4419 (1996).
[28] M. Beneke, G. Buchalla, C. Greub, A. Lenz, and U. Nierste, Phys. Lett. B **459**, 631 (1999).
[29] A. S. Dighe, T. Hurth, C. S. Kim, and T. Yoshikawa, Nucl. Phys. **B624**, 377 (2002).
[30] M. Beneke, G. Buchalla, A. Lenz, and U. Nierste, Phys. Lett. B **576**, 173 (2003).
[31] M. Ciuchini, E. Franco, V. Lubicz, F. Mescia, and C. Tarantino, J. High Energy Phys. 08 (2003) 031.
[32] A. Badin, F. Gabbiani, and A. A. Petrov, Phys. Lett. B **653**, 230 (2007).
[33] C. W. Bauer and N. D. Dunn, Phys. Lett. B **696**, 362 (2011).
[34] A. K. Alok, S. Baek, and D. London, J. High Energy Phys. 07 (2011) 111.
[35] A. Dighe, A. Kundu, and S. Nandi, Phys. Rev. D **76**, 054005 (2007).
[36] A. J. Buras, M. Jamin, and P. H. Weisz, Nucl. Phys. **B347**, 491 (1990).
[37] A. J. Buras, in *Probing the Standard Model of Particle Interactions*, edited by R. Gupta, A. Morel, E. de Rafael, and F. David (North-Holland, Amsterdam, 1999).
[38] K. Nakamura *et al.* (Particle Data Group), J. Phys. G **37**, 075021 (2010).
[39] J. Laiho, E. Lunghi, and R. S. Van de Water, Phys. Rev. D **81**, 034503 (2010).
[40] C. Csaki, A. Falkowski, and A. Weiler, J. High Energy Phys. 09 (2008) 008.
[41] G. Buchalla, A. J. Buras, and M. E. Lautenbacher, Rev. Mod. Phys. **68**, 1125 (1996).
[42] D. Becirevic, V. Gimenez, G. Martinelli, M. Papinutto, and J. Reyes, J. High Energy Phys. 04 (2002) 025.
[43] A. Abulencia *et al.* (CDF Collaboration), Phys. Rev. Lett. **97**, 242003 (2006).
[44] H. Davoudiasl, G. Perez, and A. Soni, Phys. Lett. B **665**, 67 (2008).
[45] M. Bauer, S. Casagrande, L. Grunder, U. Haisch, and M. Neubert, Phys. Rev. D **79**, 076001 (2009).
[46] A. J. Buras and D. Guadagnoli, Phys. Rev. D **78**, 033005 (2008).
[47] J. Santiago, J. High Energy Phys. 12 (2008) 046.
[48] LHCb Collaboration, Report No. LHCb-CONF-2011-049 (2011).
[49] LHCb Collaboration, Report No. LHCb-CONF-2011-051 (2011); Report No. LHCb-CONF-2011-056 (2011).
[50] D. Asner *et al.* (Heavy Flavor Averaging Group), arXiv:1010.1589.
[51] V. M. Abazov *et al.* (D0 Collaboration), Phys. Rev. D **82**, 032001 (2010).
[52] Y. Grossman, Y. Nir, and G. Raz, Phys. Rev. Lett. **97**, 151801 (2006).
[53] M. Blanke, A. J. Buras, D. Guadagnoli, and C. Tarantino, J. High Energy Phys. 10 (2006) 003.
[54] M. Bona *et al.* (UTfit Collaboration), PMC Phys. A **3**, 6 (2009).
[55] A. J. Buras, M. Misiak, and J. Urban, Nucl. Phys. **B586**, 397 (2000).
[56] J. A. Bagger, K. T. Matchev, and R. J. Zhang, Phys. Lett. B **412**, 77 (1997).
[57] A. J. Buras, M. Jamin, M. E. Lautenbacher, and P. H. Weisz, Nucl. Phys. **B400**, 37 (1993).
[58] M. Ciuchini, E. Franco, G. Martinelli, and L. Reina, Nucl. Phys. **B415**, 403 (1994).